Soft Matter

Accepted Manuscript

ROYAL SOCIETY OF CHEMISTRY

www.rsc.org/softmatter

A quantitative appraisal of the binding interactions between anionic dye, Alizarin Red S and alkyloxypyridinium surfactants: a detailed micellization, spectroscopic and electrochemical study

Renu Sharma, Ajar Kamal and Rakesh Kumar Mahajan*

*Department of Chemistry, UGC-Centre for Advanced Studies-I, Guru Nanak Dev University, Amritsar-143005, India

**To whom correspondence should be addressed:*

e-mail: rakesh_chem@yahoo.com; Fax: +91 183 2258820

Abstract

Interactions of anionic redox-active dye, Alizarin red S (ARS) with novel N-hydroxyethyl-3-alkyloxypyridinium surfactants; 1-(2-Hydroxyethyl)-3-(tetradecyloxy) pyridinium bromide, [$HEC_{14}OPyBr$] and 1-(2-Hydroxyethyl)-3-(hexadecyloxy) pyridinium bromide, [$HEC_{16}OPyBr$] were investigated in aqueous solution for the first time with an attempt to get comprehensive knowledge of oppositely charged dye-surfactant mixed systems. Different state of art techniques viz. conductivity, surface tension (ST), UV-visible, cyclic voltammetry (CV), linear sweep voltammetry (LSV), potentiometry, dynamic light scattering (DLS) and ^{1}H-NMR have been employed. The presence of ARS decreases the critical micelle concentration (*cmc*) of alkyloxypyridinium surfactants as the ARS monomers behave as aromatic counterions. A combined analysis of the techniques revealed the existence of cation-π, π-π stacking, H-bonding, electrostatic and hydrophobic interactions among ARS and alkyloxypyridinium surfactants. A quantitative appraisal of the process of interaction among ARS and alkyloxypyridinium surfactants has been made in terms of various micellar, binding and electrochemical parameters evaluated using ST, UV-visible and voltammetric measurements. Also, the results extracted from ^{1}H-NMR and voltammetric measurements indicate that the catechol moiety of ARS is involved in the binding mechanism among ARS and alkyloxypyridinium surfactants.

Keywords: Alkyloxypyridinium surfactants, cation-π interactions, linear sweep voltammetry, formal potential, ^{1}H-NMR, redox-active anionic dye.

1. Introduction

There are different types of dyes which are classified as azo, acridine, cyanine, arylmethane, anthraquinone, nitro, nitroso, thiazole and xanthenes dyes depending on the type of chromophore present in the dye molecule [1-3]. Among these dyes, anthraquinone moiety based dyes are one of the important commercial dyes owing to their diverse applications in various fields [4,5]. Alizarin red S (ARS) {Alias Mordant Red 3} with IUPAC name 1,2-dihydroxy-9,10-anthraquinone sulphonic acid sodium salt belongs to anthraquinone group of dyes. ARS has been enjoying great interest in the last few years due to its applications as a dye, staining agent for calcium in biological samples, in textile dyeing and in spectrophotometric determination of pH [6-9]. ARS can form complexes with different metal ions and shows sharp color changes due to the formation of metal-dye complex and thus, it can be used for their separation from waste water and voltammetric determination in catalysis of reaction [10-12]. ARS is used by the analysts for the detection of proteins, phenothiazine derivatives and pharmaceutical formulations [13,14]. Despite of the numerous applications of ARS, yet, very little attention has been paid to analyze its aggregation behavior.

Nowadays, the researchers are investigating new methods to develop efficient and cost effective technologies to remove environmentally harmful dyes from industrial effluents. In this regard, surfactants micelles are one of the methods to trap the hydrophobic dyes from the effluents [15]. However, the mixtures of dyes and surfactants have enormous applications in various fields of science like chemistry, biochemistry, pharmacology *etc*. Addition of minute quantity of surfactant accelerates the rate of dye adsorption onto the fibres in the textile industries. In addition to these, surfactants also act as wetting and dispersing agent for the low solubility of dyes. The spectral changes occurring in the charged dye-surfactant systems are attributed to the formation of dye-surfactant complexes, salts, ion pairs, induced self aggregation of dye, dye-rich pre-micelles and pure micelles of surfactants with solubilized monomers of dyes. These changes have been earlier observed effectively by a number of techniques such as conductometry, fluorescence spectroscopy, spectrophotometry, potentiometry and voltammetry [3,16-19] where dye-surfactant interactions were found to be influenced by the charge, alkyl chain length of surfactants and the location of the substituents on the aromatic ring of the dye molecules. Towards this strategy, very few studies concerning the interactions among ARS and

surfactants have been published so far, and accordingly, the observed facts are not so far well understood. Gul *et al.* explored the interactions among ARS and cetyltrimethylammonium bromide (CTAB) using UV-visible technique and observed that ion-pair formation took place between the dye and surfactant. They concluded that both electrostatic and hydrophobic interactions play an important role in binding among ARS and CTAB [20].

Among different types of surfactants *viz.* cationic, anionic, nonionic and zwitter-ionic, the cationic surfactants are one of the crucial class of surfactants since these have wide range of applications. Cationic surfactants are used in antibacterials, liquid crystals, oil recovery, pharmaceuticals, corrosion inhibitor, in road pavement, food industries and other aspects of materials science [21]. Recently, they are also being used as soft templates for the synthesis of mesoporous materials, capping agent for the synthesis of nanoparticles and nanorods, and biomedical applications including gene or drug delivery [22-24]. Pyridinium Cationic surfactants are a peculiar class of surfactants and their surface properties and characteristics have been thoroughly studied. In the present study, we have employed new N-hydroxyethyl-3-alkyloxypyridinium surfactants, 1-(2-Hydroxyethyl)-3-(tetradecyloxy) pyridinium bromide, [HEC_{14}OPyBr] and 1-(2-Hydroxyethyl)-3-(hexadecyloxy) pyridinium bromide, [HEC_{16}OPyBr]. These surfactants possess very low critical micelle concentration (*cmc*) values as compared to pyridinium, imidazolium, and conventional cationic surfactants. They have very low cytotoxicity than conventional surfactants as assessed by MTT assay on C6 glioma cells and thermally stable upto 230°C [25].

In view of various applications of the dye-surfactant mixed systems and the unique characteristics of these novel alkyloxypyridinium surfactants, the present work is mainly focused to explore the physicochemical behavior of these surfactants during their interaction with anthraquinone moiety based anionic dye, alizarin red S (ARS). Cyclic voltammetry (CV), linear sweep voltammetry (LSV) and ^{1}H-NMR techniques provides detailed insights of the mechanism behind the interactions among ARS and alkyloxypyridinium surfactants. Along with these studies, surface tension and conductivity measurements have been done to evaluate micellar, interfacial and thermodynamic parameters. Binding constant (k) and free energy change (ΔG) for the dye-surfactant mixed systems are calculated using spectroscopic and voltammetric techniques. Further, electrochemical parameters of ARS like diffusion coefficient (D), formal

charge ($E°$) electron transfer coefficient (α) and surface reaction rate constant (k_s) have been evaluated in the absence and presence of alkyloxypyridinium surfactants. The microstructures of dye-surfactant complexes are elucidated using dynamic light scattering (DLS) technique.

2. Experimental Section

2.1 Materials and methods

The alkyloxypyridinium surfactants, 1-(2-Hydroxyethyl)-3-(tetradecyloxy) pyridinium bromide and 1-(2-Hydroxyethyl)-3-(hexadecyloxy) pyridinium bromide were synthesized as described elsewhere [25]. Alizarin red S (ARS) with 98% purity was purchased from Sigma Aldrich. The plasticizer, bis (2-ethyl-hexyl) phthalate (DOP) was a product of Qualigens, India. All chemicals used were of analytical grade and used as received. Double distilled water was used in preparing all the solutions. A sartorius analytical balance with a precision of ±0.0001 g was used for weighing purpose. Various techniques such as conductivity, surface tension, UV-visible, cyclic voltammetry (CV), linear sweep voltammetry (LSV), potentiometry, dynamic light scattering (DLS) and ^{1}H-NMR have been employed. The annexure describing the methodology employed for various measurements in detail is provided as Annexure SI (supporting information). The pK$_a$ value of ARS is 5.5. If pH > 5.5, ARS exists in mono-anionic form and the surfactants employed in the present work are mono-cationic. Therefore, aqueous medium (pH 7.0) has been chosen as a medium for all the techniques employed. All the measurements were performed in triplicate at 25±0.1°C.

3. Results and discussion

3.1 Conductivity measurements

In order to consider the effect of ARS on the aggregation behavior of alkyloxypyridinium surfactants, conductivity measurements have been performed as a function of concentration of [HEC$_{14}$OPyBr] and [HEC$_{16}$OPyBr] in the absence and presence of varying amounts of ARS [0.02, 0.05, 0.075 and 0.1 mmol dm^{-3}]. As shown in Fig.1 and Fig.S1(A) (supporting information), the change in conductivity values for pure [HEC$_{14}$OPyBr] and [HEC$_{16}$OPyBr] fit into two straight lines of different slopes and the point of intersection of the tangent lines of the abrupt change in slopes gives the value of *cmc*. The *cmc* values of pure alkyloxypyridinium surfactants match well with their literature values [25] and the values are given in Table 1. It can be seen that the addition of ARS brings out significant changes in the conductivity profiles of

alkyloxypyridinium surfactants. The conductivity profiles of surfactants in the presence of ARS show three lines of different slopes whose intersection points correspond to two transitions designated as C_1 where oppositely charged ion-pairs of ARS and surfactants are formed and C_2 (*cmc*) where free micelle formation of alkyloxypyridinium surfactants takes place [as shown in Fig.1]. Initially, on addition of alkyloxypyridinium surfactants where they are present in monomeric form, the interactions between positively charged monomers of surfactants and negatively charged ARS molecules starts and it results in the formation of ion-pairs due to strong electrostatic forces of attraction.

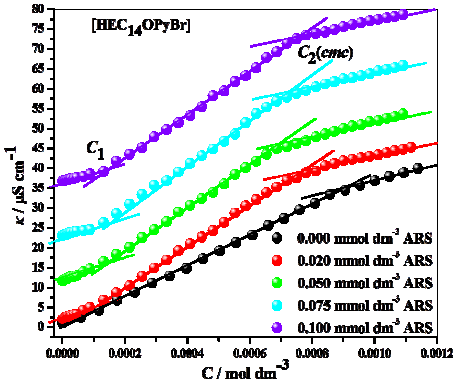

Fig.1 Variation of specific conductivity (κ) with molar concentration of alkyloxypyridinium surfactant, [$HEC_{14}OPyBr$] in the absence and presence of varying amounts of ARS.

This ion-pair formation gives rise to a transition designated as C_1 (shown in Fig.1) and this concentration corresponds to 1:1 stoichiometry of the oppositely charged ARS-surfactant ion-pair complexes. This concentration corresponds to same one where first minimum appears in the tensiometric profiles (discussed later). Further, conductivity increases but with a smaller slope than the former and concentration of free monomers of surfactants attains a threshold value which micellization of alkyloxypyridinium surfactants occur. The *cmc* values of alkyloxypyridinium surfactants are found to be lower in the presence of anionic dye, ARS. Such behavior has been reported earlier for oppositely charged dye and surfactant mixed systems [21,26]. Beyond *cmc*, free micelles of alkyloxypyridinium surfactants are formed with dye monomers solubilized in the outer portion of micelles as it is expected due to decrease in *cmc* values of alkyloxypyridinium surfactants in the presence of ARS. The degree of counter-ion binding (β) provides the average number of counter-ions per surfactant ion in the micelle and is

related to related to degree of dissociation (α) as β = 1-α, where α is obtained by the ratio of slopes of post to pre-micellar region.

Employing the charged pseudophase model of micelle formation [27] and using the value of β, the standard free energy of micellization per mole of surfactant ($\Delta G°_{mic}$), is calculated as per the equation (1):

$$\Delta G°_{mic} = (1+\beta)\, RT \ln X_{cmc} \quad (1)$$

Where X_{cmc}, R and T denote *cmc* of surfactants expressed in mole fraction units, gas constant and temperature on Kelvin scale respectively. The values of $\Delta G°_{mic}$ and β are given in Table 1.

Table1. Micellization parameters of alkyloxypyridinium surfactants [$HEC_{14}OPyBr$] and [$HEC_{16}OPyBr$] in the presence of varying amounts of ARS (C_{ARS}); concentration corresponding to ion-pair formation (C_1), critical micelle concentration (C_2(*cmc*)), degree of counter ion binding (β) and standard free energy of micellization ($\Delta G°_{mic}$) as determined from conductivity measurements.

[$HEC_{14}OPyBr$]				
C_{ARS}(mmol dm^{-3})	C_1(mmol dm^{-3})	C_2 = *cmc*(mmol dm^{-3})	β	$-\Delta G°_{mic}$(kJ mol^{-1})
0.000	-	0.88	0.42	38.9
0.020	-	0.71	0.44	40.2
0.050	0.06	0.72	0.47	41.0
0.075	0.08	0.74	0.54	42.8
0.100	0.09	0.76	0.61	45.5
[$HEC_{16}OPyBr$]				
C_{ARS}(mmol dm^{-3})	C_1(mmol dm^{-3})	C_2 = *cmc*(mmol dm^{-3})	β	$-\Delta G°_{mic}$(kJ mol^{-1})
0.000	-	0.19	0.45	45.2
0.020	0.02	0.14	0.53	48.9
0.050	0.04	0.15	0.56	49.5
0.075	0.06	0.17	0.58	49.7
0.100	0.07	0.18	0.64	51.3

The error estimate in *cmc* is ±0.006 mmol dm^{-3}

The β values increase with the increase in alkyl chain length of surfactants both in the absence and presence of ARS which is in accordance with the literature [28]. The values of $\Delta G°_{mic}$ are found to be negative which indicate the spontaneity of the micellization process. The negative values of $\Delta G°_{mic}$ increase on increasing the dye content in mixed systems which further suggest that micelle formation becomes more feasible with increase in dye content. However, more negative values obtained for ARS-[HEC_{16}OPyBr] mixed system suggests the greater feasibility of micellization process by virtue of more hydrophobic interactions.

3.2 Surface activity of dye-surfactant mixed system

The formation of surface active dye-surfactant aggregates in bulk also affects the structure of surface monolayer leading to manifest changes in surface tension profiles of dye-surfactant mixed systems. The variation in surface tension, γ of alkyloxypyridinium surfactants in the absence and presence of 0.02 mmol dm^{-3} of ARS are shown in Fig.2 and Fig.S1(B) (supporting information) for [HEC_{14}OPyBr] and [HEC_{16}OPyBr], respectively. In the absence of dye, γ decreases gradually on increasing the amount of alkyloxypyridinium surfactants and levels off at certain concentration which is termed as critical micelle concentration (*cmc*). The *cmc* values of pure surfactants are in accordance with the literature [25] and are given in Table 2. The presence of ARS enhances the propensity of surfacatnt molecules to migrate to solution surface leading to decrease in γ at much lower concentration of alkyloxypyridinium surfactants. Such behavior is due to the formation of more hydrophobic dye-surfactant ion-pairs at the surface among the oppositely charged dye and surfactant monomers attributable to the mutual effect of hydrophobic and electrostatic interactions.

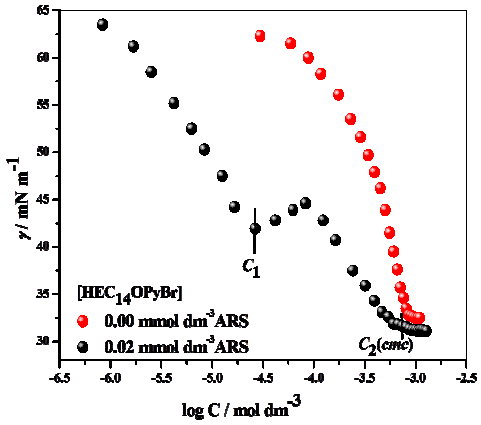

Fig.2 Variation of surface tension (γ) as a function of logarithm of molar concentration of alkyloxypyridinium surfactant, [HEC_{14}OPyBr] in the absence and presence of 0.02 mmol dm^{-3} ARS

As the concentration of [HEC_{14}OPyBr] reaches 0.03 mmol dm^{-3}, the surface is saturated by these ion-pairs. This concentration is designated as C_1 where dye-surfactant ion-pairs are formed. The efficiency of a surfactant (pC_{20}) to reduce γ is described in terms of negative logarithm of C_{20}, where C_{20} denotes the concentration of surfactant required to reduce the surface tension of pure solvent by 20 mN m^{-1}. The larger pC_{20} value indicates higher adsorption efficiency for the surfactant and it depends on its hydrophobicity. As can be seen from Table 2, the pC_{20} values increase with the chain length of alkyloxypyridinium surfactants both in the absence and presence of ARS *i.e.* it is found to be more in case of [HEC_{16}OPyBr]. This increase in efficiency of surfactants in the presence of dye is due to the formation of close-packed dye-surfactant ion pairs (DSIP) that act as a non-ionic surfactant with larger head group *i.e.* ARS molecules behave as aromatic anions and the non-ionic surfactants have usually higher efficiency than ionic ones [27]. Also, the DSIP formation occurs due to specific interaction among them which exists in the ion-pair monolayer at the air-solution interface and it ultimately affects the tensiometric profiles of alkyloxypyridinium surfactants. Further, a slight increase in γ of 2-3 mN m^{-1} has been observed with increase in concentration of both alkyloxypyridinium surfactants due to transformation of non-ionic DSIP to cationic form. This surface saturation by dye-surfactant ion-pairs has been reported in similar systems [29]. More addition of [HEC_{14}OPyBr] results in further decrease of γ and aggregates of dye and surfactants gets dissociated and micelles of pure surfactants with monomers of dye associated near the micellar surface are formed. Similar changes have been observed in the ARS-[HEC_{16}OPyBr] mixed system.

Various interfacial and thermodynamic parameters like surface tension at *cmc* (γ_{cmc}), maximum surface excess concentration at the air-solution interface (Γ_{max}), minimum area per molecule (A_{min}), effectiveness of surface tension reduction (π_{cmc}), Gibbs free energy of adsorption (ΔG°_{ads}) (using ΔG°_{mic} from conductivity at 298.15K) have been calculated using the standard equations (Annexure SII, supporting information) and are given in Table 2. π_{cmc} indicates the maximum reduction of surface tension due to the dissolution of surfactant molecules and hence becomes a measure for the effectiveness of the surfactant to lower the surface tension of the solvent. The π_{cmc} values increase in the presence of dye for both the surfactants which suggests that DSIP are more effective in lowering the surface tension. The Γ_{max}

values of alkyloxypyridinium surfactants have been found to decrease in the presence of dye. Alternatively, the A_{min} values increases by approximately 30% in the presence of dye. It indicates that larger surface area is required for DSIP than the surfactant alone. In addition to this, the DSIP formation is equivalent to the formation of a new non-ionic surfactant with a larger head group and as a result a larger surface area per surfactant leads to lower *cmc* of ion-pair surfactant [30]. The ΔG°_{ads} values are found to be negative indicating the spontaneity of adsorption process. However, the values of ΔG°_{ads} become more negative with the increase in hydrophobicity of surfactants both in the absence and presence of ARS.

Table 2. Interfacial parameters *i.e.* surface tension at *cmc* (γ_{cmc}), effective surface tension reduction (Π_{cmc}), surface excess (Γ_{max}), minimum area per molecule (A_{min}) and Gibbs free energy of adsorption (ΔG°_{ads}) of alkyloxypyridinium surfactants, [HEC_{14}OPyBr] and [HEC_{16}OPyBr] in the absence and presence of 0.02mmol dm^{-3} ARS at 298.15K.

	cmc (mmol dm^{-3})	γ_{cmc} (mN m^{-1})	π_{cmc} (mN m^{-1})	pC_{20} (mmol dm^{-3})	$\Gamma_{max} \times 10^6$ (mol dm^{-3})	A_{min} ($Å^2$)	ΔG°_{ads} kJ mol^{-1}
			In water				
[HEC_{14}OPyBr]	0.87	32.8	40.1	3.64	4.49	36.0	-47.8
[HEC_{16}OPyBr]	0.21	38.6	34.2	4.17	2.94	56.5	-70.4
			In 0.02 mmol dm^{-3} ARS				
[HEC_{14}OPyBr]	0.73	31.4	41.4	5.21	1.37	121.0	-56.8
[HEC_{16}OPyBr]	0.16	37.3	35.5	5.57	0.85	195.0	-90.7

The error estimate in *cmc* is ±0.006 mmol dm^{-3}

3.3 Spectroscopic studies

3.3.1 Effect of pH on the absorption spectrum of alizarin red S

UV-visible spectrum of alizarin red S (ARS) is highly dependent on pH of the solution due to the presence of two replaceable protons of hydroxyl groups [16]. The pKa values of ARS are 5.5 and 11.0. At pH < 5.0, ARS exists as neutral molecule, while at pH > 9.0; it is present in

dianionic form. In between this range *i.e.* from 5.5 to 9.0, it exists in mono-anionic form. These different forms of ARS are presented in Scheme 1.

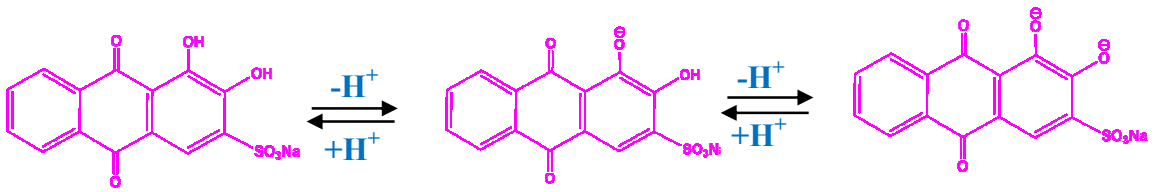

(A) Neutral form of ARS (B) Monoanionic form of ARS (C) Dianionic form of ARS

Scheme 1 Molecular structures of Alizarin red S (ARS): (A) Neutral form of ARS (B) Monoanionic form of ARS (C) Dianionic form of ARS.

ARS shows absorption band at 421, 423 and 518.5 nm at a pH of 4.0, 7.0 and 10.0 corresponding to neutral, mono-anionic and di-anionic forms of ARS, respectively. In acidic medium (pH 4.0), ARS exists in protonated form and the reaction is very slow to be observed. In neutral aqueous medium (pH 7.0), deprotonation of one of the hydroxyl group takes place and thus, intramolecular hydrogen bonding occurs between other hydroxyl group and ketonic oxygen, thus forming a six membered ring. The absorption spectrum of ARS in neutral aqueous medium (pH 7.0) shows two absorption bands at 335 and 423 nm which are due to n→π^* transitions of p-benzoquinone group (diketo form) condensed between two rings. In basic medium (pH 10), the dianionic form of ARS shows absorption band at 518.5 nm. This large bathochromic shift from 423 to 518.5 nm is due to extensive delocalization of electrons that reduces the required energy for transition and thus shifts the absorption band towards longer wavelength. In the present study, the UV-visible absorption spectrum of ARS in water has been recorded in the concentration range of 10^{-3} mol dm^{-3} to 10^{-6} mol dm^{-3} where it strictly follows Lambert-Beer's law *i.e.* absorbance increases with the increase in concentration of dye.

3.3.2 Interactions between ARS and alkyloxypyridinium surfactants

In this section, the spectral variation of ARS with increasing concentrations of alkyloxypyridinium surfactants, [HEC_{16}OPyBr] and [HEC_{16}OPyBr] has been explored. The UV-visible spectra of 0.02 mmol dm^{-3} ARS in the presence of varying amounts of [HEC_{14}OPyBr] and [HEC_{16}OPyBr] are shown in Fig.3(A) and Fig.S2(A) [supporting information]. The gradual addition of alkyloxypyridinium surfactants up to a concentration of 0.03 mmol dm^{-3} (which is in accordance with C_1 as observed in conductivity and ST measurements) is seen to bring about a

small increase in intensity without shift in wavelength of maximum intensity (λ_{423}). The strong electrostatic binding between oppositely charged ARS and alkyloxypyridinium surfactants led to the formation of ion-pairs among them. This is an unusual spectroscopic behavior observed in the present study, as in most of the anionic dye-cationic surfactant mixed systems, the intensity initially decreases on the addition of surfactants [31,32]. The formation of ion-pairs reduces the electrostatic repulsions among the dye molecules and they approach each other by means of both electrostatic interactions and hydrophobic interactions. In addition to these interactions, the presence of hydrogen bonding among carbonyl oxygen of anthraquinone moiety and hydroxyl group of alkyloxypyridinium bromide surfactants also play an important role. Fig.3(B) and Fig.S2(B) (supporting information) depicts the variation of absorbance and wavelength corresponding to maximum intensity (λ_{max}) of ARS as a function of concentration of [HEC_{14}OPyBr] and [HEC_{16}OPyBr] respectively. Initially, as compared to the absorbance, the wavelength corresponding to maximum intensity is not much affected by the addition of surfactants. Further, absorbance and λ_{max} show opposite behavior with the increase in concentration of alkyloxypyridinium surfactants. On one hand, the absorbance shows marked decrease, whereas on the other hand, λ_{max} shows large bathochromic shift of 130.5 nm (423 nm to 553.5 nm). This large shift is associated with the formation of a new absorption band at 553.5 nm. This strong shift of 130.5 nm in absorption maximum may be due to the charge transfer interactions and strong electronic coupling between anionic dye and cationic alkyloxypyridinium surfactants in which ARS acts as acceptor and alkyloxypyridinium surfactant as donor one. These results are also verified by voltammetric and NMR measurements discussed in the forthcoming sections. This transition is also revealed by the isosbestic point at 474 nm which gets red shifted with increasing concentration of alkyloxypyridinium surfactants. The formation of surfactant premicelles or dye-surfactant aggregates increases the hydrophobicity of the medium due to which the absorption band (due to $n\rightarrow\pi^*$) gets red-shifted, since the $n\rightarrow\pi^*$ transitions usually show bathochromic shift with the decrease in polarity of the medium. The visual change in the color of the dye (light yellow to purple) (shown in inset of Fig.3(A)) has been observed on the addition of alkyloxypyridinium surfactants which strongly indicates the dye-surfactant complexation. Above *cmc*, the absorption spectra of ARS do not any change with

the addition of alkyloxypyridinium surfactants which suggests the formation of mixed micelles of alkyloxypyridinium surfactants with intercalation of ARS monomers.

To confirm the formation of dye-surfactant complexes and to determine the stoichiometric ratio of ion-pairs of ARS and alkyloxypyridinium surfactants, the method of continuous variation (Job's method) has been used. In this method, various volume fractions of equimolar solutions of dye and alkyloxypyridinium surfactants (1.0 mmol dm^{-3} of aqueous mixtures of each of dye and surfactants were used in the present study) were mixed and the corrected absorbances of these mixtures (ΔA) were plotted against the volume fraction of alkyloxypyridinium surfactant solution (X).

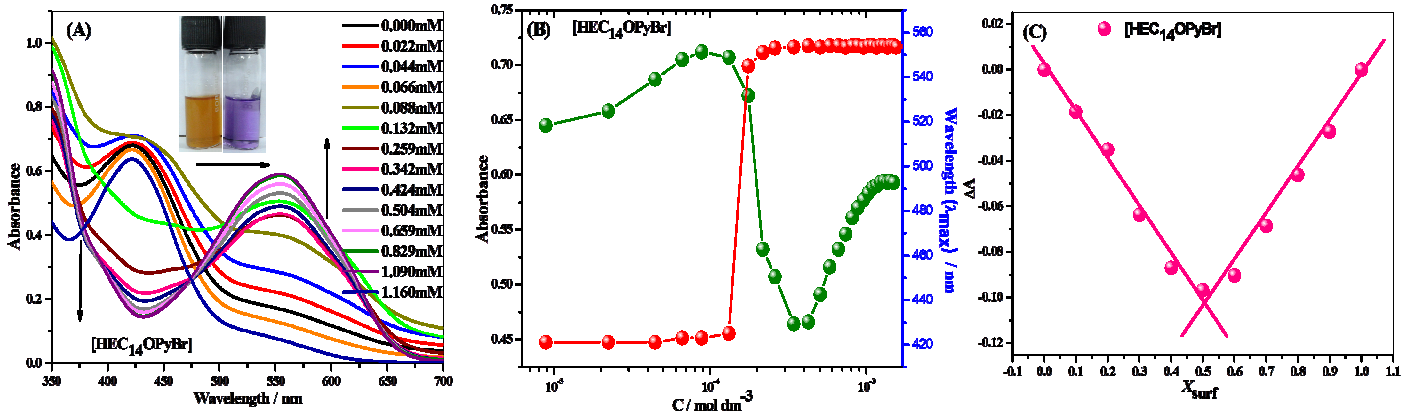

Fig.3 (A) UV-visible spectrum of 0.02 mmol dm^{-3} ARS in the presence of increasing concentrations of alkyloxypyridinium surfactant, [HEC_{14}OPyBr] (B) Plot of Absorbance and λ_{max} *versus* increasing concentration of [HEC_{14}OPyBr] (C) Job's plot depicting 1:1 stoichiometry of ARS-[HEC_{14}OPyBr] mixed system.

The maximum/minimum occurs at volume ratio $X = X_m$, that corresponds to the combining ratio of dye and surfactant in the complex. Fig.3(C) and Fig.S2(C) (supporting information) depict the variation of corrected absorbances (ΔA) *versus* volume fraction of alkoxypyridinium surfactants. The corrected absorbance (ΔA) represents the difference between the measured absorbance (A_{exp}) and theoretical absorbance (A_{theo}) as per the equation (2) [33]

$$\Delta A = A_{exp} - A_{theo} \quad (2)$$

Where A_{theo} is calculated taking into account the Beer-Lambert's law *i.e.* the two components do not interact with each other and hence the total absorbance of the mixture is equal to the sum of their individual absorbances according to the equation (3)

$$A_{Theo} = \varepsilon_S C_S^0 X_S - \varepsilon_D C_D^0 (1 - X_S) \quad (3)$$

Here, ε_s and ε_D are the molar extinction coefficients and C_s^0 and C_D^0 are the concentrations of the stock solutions of the alkyloxypyridinium surfactants and the dye (ARS) respectively, whereas, X_s represents the volume fraction of alkyloxypyridinium surfactants. The formation of dye-surfactant complexes makes the absorbance of the solution to satisfy the following equation (4):

$$A_{exp} = \varepsilon_S C_S + \varepsilon_D C_D + \varepsilon_{S-D} C_{S-D} \quad (4)$$

Where $\varepsilon_{S\text{-}D}$ *is* the molar extinction coefficient of the dye-surf complex and C_S, C_D and $C_{S\text{-}D}$ are the concentrations of the respective species in the mixture. As depicted in Fig. 3(C) and Fig.S2(C) (supporting information), the presence of a minimum in the Job's plot for the dye-surfactant mixtures at $X_S \approx 0.5$ corresponds to 1:1 stoichiometry for their binding. Further it also validates the presence of only one complex species in the solution.

To estimate the interactions among ARS and alkyloxypyridinium surfactants quantitatively, binding constant has been calculated by the use of modified BH equation (5) [34]:

$$\frac{1}{\Delta A} = \frac{1}{\Delta A_{max}} + \frac{1}{k_a \Delta A_{max} [Surf]^n} \quad (5)$$

Where $\Delta A = A_0 - A$; A_0 and A represent the absorbance of 0.02 mmol dm^{-3} aqueous ARS solution at 423 nm in the absence and presence of alkyloxypyridinium surfactants respectively, [Surf] denotes the molar concentration of the alkyloxypyridinium surfactants viz. [HEC_{14}OPyBr] and [HEC_{16}OPyBr] and n is the stoichiometric coefficient. In the present study, the double reciprocal plot of $1/ A_0\text{-}A$ and 1/[Surf] shows linearity which also confirms the formation of 1:1 ion-pair complex between ARS and alkyloxypyridinium surfactants [Fig.S6(A) supporting information]. These results are in accordance with the conductivity measurements. Using the value of binding constant k_a, the Gibbs free energy change for dye-surf complexes has been evaluated by employing the equation (6).

$$\Delta G = -RTlnk_a \quad (6)$$

The values of binding constant (k_a) and Gibbs free energy (ΔG) so obtained are given in Table 3. The negative values of Gibbs free energy indicate the spontaneity of complexation

among ARS and alkyloxypyridinium surfactants. The magnitude of k_a and ΔG for [HEC_{16}OPyBr] are found to be more than [HEC_{14}OPyBr] which indicates more stability and spontaneity of ion-pair formation with the former due to more hydrophobic interactions.

Table 3. Binding constants (k_a), correlation coefficients (R_c) and corresponding free energy change of binding (ΔG) for ion-pair complex formation between ARS and alkyloxypyridinium surfactants, [HEC_{14}OPyBr] and [HEC_{16}OPyBr] evaluated from UV-visible and voltammetric measurements

System	k_a ($\times 10^3$ M^{-1})	R_c	ΔG (kJ mol^{-1})
Absorbance			
ARS + [HEC_{14}OPyBr]	2.82	0.976	-19.7
ARS + [HEC_{16}OPyBr]	5.23	0.998	-21.2
Voltammetric			
ARS + [HEC_{14}OPyBr]	2.26	0.995	-19.1
ARS + [HEC_{16}OPyBr]	4.62	0.994	-20.9

3.4 Electrochemical studies

3.4.1 Cyclic Voltammetric (CV) measurements

Alizarin red S (ARS) is an electroactive dye due to the presence of two hydroxyl groups on anthraquinone moiety. Alizarin red S has two sites where redox changes can occur. The redox activity can occur at positions 9 and 10, *i.e.* anthraquinone moiety of the central ring leading to formation of hydroquinone derivative, or at the catecholic moiety at the positions 1 and 2 as presented in Scheme 2 [36].

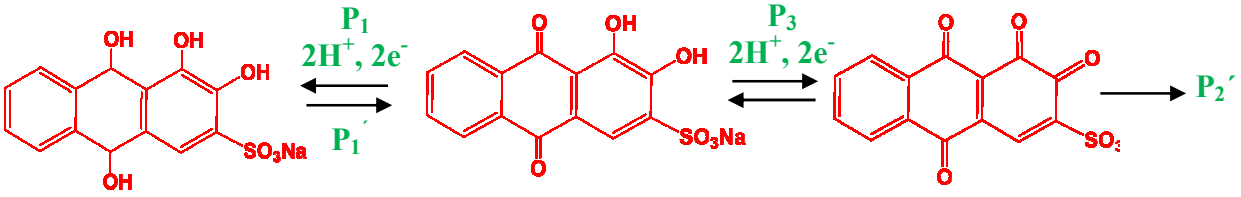

Scheme 2 Schematic presentation of possible electrochemical oxidation and reduction processes in ARS.

ARS exhibits two oxidation peaks (P_1) and (P_3) at -0.54 V and 0.42 V, two reduction peaks (P_1') and (P_2') at -0.64 V and -0.24 V as per the literature reports [35]. The first redox

peaks P_1 and P_1' showed a quasi-reversible voltammetric response corresponding to the redox reaction of anthraquinone [36]. The anodic peak P_3 corresponds to the oxidation of catechol moiety that occurs at a very high potential as compared to the other peak and no well defined reduction peak corresponding to P_3 could be obtained. Therefore, it is an irreversible electrochemical process. In the present study, CV of ARS (0.02 mmol dm^{-3}) run in 0.1 M phosphate buffer of pH 7.4 as a supporting electrolyte in the potential range of -0.8 to 1.4 V *versus* Ag/Ag^+ are shown in Fig.4(A). ARS exhibited two oxidation peaks P_1 and P_3 at potential of -0.627 V and 0.335 V *versus* Ag/Ag^+ in the first sweep segment (lower to higher potential) and two reduction peaks P_1' and P_2' appear at potentials of -0.732 and -0.328 V *versus* Ag/Ag^+ in the second sweep segment (higher to lower potential) (shown in Fig.4(A)) which are in very good agreement with the literature [36].

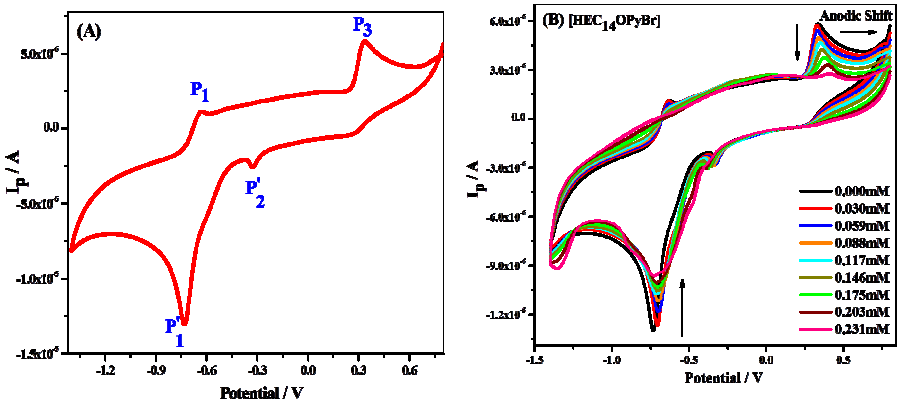

Fig.4 (A) Cyclic voltammogram of 0.02 mmol dm^{-3} ARS (B) Cyclic voltammograms of ARS in the presence of increasing concentrations of [HEC_{14}OPyBr].

In CV measurements, the addition of alkyloxypyridinium surfactant [HEC_{14}OPyBr] to 0.02 mmol dm^{-3} ARS led to anodic shift (increase in potential) of reduction peak P_1' from -0.732 V to -0.698 V and oxidation peak P_3 from 0.335V to 0.408 V along with decrease in current intensities [shown by arrows in Fig.4(B)]. Similar changes have been observed in ARS-[HEC_{16}OPyBr] mixed system [Fig.S3(A)]. This substantial shift in potential and decrease in peak current could be due to formation of non-electroactive dye-surfactant complex resulting in overall decrease in concentration of electroactive dye molecules. However, it is clear from voltammetric measurements that more prominent changes are observed in the oxidation peak P_3.

To get better resolution of this peak, we carried out Linear Sweep Voltammetry (LSV) of ARS in the absence and presence of alkyloxypyridinium surfactants under similar conditions. In LSV studies also, the potential of oxidation peak P_3 shifts towards more positive potential (anodic shift) with a decrease in current intensity with the addition of alkyloxypyridinium surfactants. The clear picture of the electrochemical changes is shown in inset of Fig.5(A) and Fig.S3(B) for ARS-[$HEC_{14}OPyBr$] and ARS-[$HEC_{16}OPyBr$] mixed systems in the potential range of -0.2 V to 0.8 V *versus* Ag/Ag^+. Both of the studies evidenced the complexation among ARS and surfactant molecules by virtue of electrostatic and hydrophobic interactions. The more pronounced changes observed in the oxidation peak P_3 *i.e.* the observed anodic shift (increase in potential) indicated that the oxidation of catechol moiety becomes difficult and we have to apply more potential in order to get the same voltammogram. This suggests that owing to the complexation among ARS and alkyloxypyridinium surfactants, the electrons are not easily available and thus, the oxidation peak shifts towards higher potential. It suggests that the hydroxyl groups of anthraquinone moiety at 1,2 position interact with alkyloxypyridinium surfactants. Such changes may be due to the charge transfer complexation as proposed in the UV-visible studies and this is supported by CV measurements.

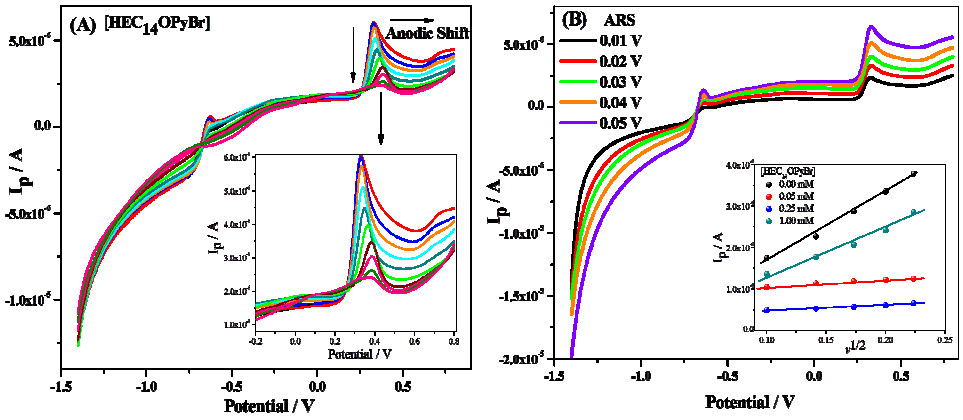

Fig.5 (A) Linear sweep voltammograms (LSV) of ARS in the presence of increasing concentrations of alkyloxypyridinium surfactant, [$HEC_{14}OPyBr$] (B) LSV of 0.02 mmol dm^{-3} ARS at various scan rates of potential [Inset of plot shows the variation of I_p (A) *versus* $v^{1/2}$ for ARS in the absence and presence of increasing concentrations of [$HEC_{14}OPyBr$].

The band gap between lower energy HOMO and higher energy LUMO is calculated using Tauc model equation [37] and is found to be 2.549 eV, 1.866 eV and 1.865 eV for ARS, ARS-[HEC_{14}OPyBr] and ARS-[HEC_{16}OPyBr] mixed systems. The band gap decreases in the presence of alkyloxypyridinium surfactants which is anticipated for the large bathochromic shift (observed in UV-visible studies). The formation of dye-surfactant charge transfer complex facilitates the jumping of electrons from lower energy HOMO (E_{HUMO} = -5.173 eV) to higher energy LUMO (E_{LUMO} = -3.307 eV) of ARS-[HEC_{14}OPyBr] in comparison to the higher energy LUMO of pure ARS (E_{LUMO} = -2.600 eV). The calculated values are given in Table 4 and the evident picture of the changes is shown in Fig.6. This reveals that the formation of charge transfer complex stabilizes the higher energy LUMO, since its energy decreases in the presence of alkyloxypyridinium surfactants. This charge transfer mechanism is also justified by the upfield shifts observed for one of the –OH groups of ARS in the ^{1}H-NMR measurements (discussed later).

Table 4. Oxidation potential corresponding to anodic peak (P_3), band gap, HOMO and LUMO values of ARS in presence of alkyloxypyridinium surfactants, [HEC_{14}OPyBr] and [HEC_{16}OPyBr]

System	Band Gap (eV)	HOMO (eV)	LUMO (eV)
ARS	2.549	-5.148	-2.600
ARS + [HEC_{14}OPyBr]	1.866	-5.173	-3.307
ARS + [HEC_{16}OPyBr]	1.865	-5.156	-3.290

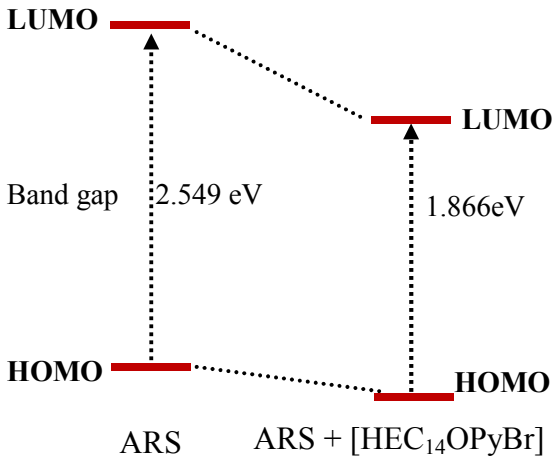

Fig.6 HOMO and LUMO values of ARS in the presence of alkyloxypyridinium surfactant, [HEC_{14}OPyBr]

3.4.2. Electrochemical parameters of ARS in the absence and presence of alkyloxypyridinium surfactants.

The effect of scan rate of potential on the electroactivity of ARS has been studied using LSV by varying the scan rates from 0.01 to 0.05 Vs^{-1}. The peak currents of ARS increase with increase in scan rates. The linear variation of current with scan rate suggests that process is diffusion controlled and provides basis to determine diffusion coefficient for the pure dye and dye-surfactant mixed systems using Randles-Sevcik equation [38] which is related to the peak current (I_p) and scan rates ($v^{1/2}$). Fig.5(B) shows the effect of scan rate of potential of the peak current of linear sweep voltammogram of ARS and the inset of the plot gives variation of I_p (A) *versus* $v^{1/2}$ for ARS in order to find the diffusion coefficients. The corresponding plots for mixed systems of ARS and alkyloxypyridinium surfactants are shown in Fig.S4 and Fig.S5 (supporting information). In the present study, diffusion coefficients of pure ARS and ARS-surfactant mixed systems have been elucidated by examining the peak current of oxidation peak P_3. The diffusion coefficient of pure dye, ARS has been found to be 17.8 $\mu cm^2\ sec^{-1}$. The distribution of ARS in aqueous and micellar phase greatly affects its diffusion due to which the addition of alkyloxypyridinium surfactants noticeably changes its diffusion coefficient. The corresponding values of ARS in the presence of 0.05 mmol dm^{-3}, 0.25 mmol dm^{-3} and 1.0 mmol dm^{-3} of [HEC_{14}OPyBr] are 1.58 $\mu cm^2\ sec^{-1}$, 1.30 $\mu cm^2\ sec^{-1}$ and 1.17 $\mu cm^2\ sec^{-1}$ respectively. The diffusion coefficients for ARS are found to be 12.1 $\mu cm^2\ sec^{-1}$, 6.73 $\mu cm^2\ sec^{-1}$ and 6.47 $\mu cm^2\ sec^{-1}$ in the presence of 0.01 mmol dm^{-3}, 0.1 mmol dm^{-3} and 0.35 mmol dm^{-3} concentrations of [HEC_{16}OPyBr], respectively. The diffusion coefficients values decrease in both of the mixed systems at all the concentrations of alkyloxypyridinium surfactants. These results clearly indicate that the decrease in current of ARS is due to binding of ARS with alkyloxypyridinium surfactants that leads to lowering of diffusion coefficient values. For diffusion controlled irreversible process, the electrochemical parameters like surface reaction rate constant (k_s) and electron transfer coefficient (α) can be calculated using the following equation (7) [39].

$$E_p = E^{\circ} + \left[0.780 + 0.5\ \ln\left({}^{m\alpha DFv}/_{RT}\right) - \ln k_s\right] {}^{RT}/_{m\alpha F} \qquad (7)$$

Where E_p is the peak potential, $E°$ is formal potential, m, R, T and F denote number of electrons, gas constant, temperature in Kelvin scale and Faraday's constant, respectively. There is a linear relation between E_p and v and the value of y-intercept obtained by extrapolating the line to $v = 0$, gives the value of formal potential ($E°$). Also, there exists a linear relation between E_p and logarithm of scan rate (ln v). The α and k_s values can be obtained from slope and intercept

of the straight line if m, D, and $E°$ are known. The values of these parameters so obtained of ARS in the absence and presence of alkyloxypyridinium surfactants are listed in Table 5. The values of electron transfer coefficient (α) decreases in the presence of alkyloxypyridinium surfactants which is in accordance with the variation of diffusion coefficient of ARS in the presence of both the surfactants (1.0 mmol dm^{-3} and 0.35 mmol dm^{-3}). This indicated that the complex formation among dye and surfactant molecules decreases the diffusion of electroactive dye molecules towards the electrode surface and as a result, the rate of electron transfer towards the electrode surface decreases. This overall leads to decrease in current intensities in voltammetric measurements.

3.4.3. Measurement of binding constant and stoichiometry of complex by Voltammetry

The modified BH equation was applied to determine the stoichiometry, binding constant (k_a) and change in free energy (ΔG) of the formation of dye-surfactant complex in voltammetric studies similar to that of UV-visible measurements. The linear decrease in peak currents has been used to evaluate binding constant by using the following equation (8) [34]:

$$\frac{1}{\Delta I_p} = \frac{1}{\Delta I_{p\,max}} + \frac{1}{k_a \Delta I_{p\,max}\,[Surf]^n} \qquad (8)$$

Where $\Delta I_p = I_0 - I$; I_0 and I represent the peak current of 0.02 mmol dm^{-3} aqueous ARS solution in the absence and presence of alkyloxypyridinium surfactants, respectively and other terms carry their usual meanings. The double reciprocal plot of $1/\Delta I_p$ *vs* 1/[Surf] shows linearity which also confirms the formation of 1:1 ion-pair complex between ARS and alkyloxypyridinium surfactants by voltammetry [Fig.S6(B) supporting information].

Table 5. Diffusion coefficient (D), formal potential ($E°$), electron transfer coefficient (α) and surface reaction rate constant (k_s) for ARS and ARS-alkyloxypyridinium surfactants, [$HEC_{14}OPyBr$] and [$HEC_{16}OPyBr$] evaluated from Linear Sweep Voltammetry (LSV) measurements.

System	D/ µcm^2 sec^{-1}	$E°$ / V	α	k_s (× 10^3) / s^{-1}
ARS	17.8	0.39	1.16	24.5
ARS + [$HEC_{14}OPyBr$]	1.17	0.29	0.37	24.0
ARS + [$HEC_{16}OPyBr$]	6.47	0.32	0.93	17.0

The calculated values of ΔG and k_a are provided in Table 3. The negative values of ΔG indicate the spontaneity of binding process. The high values of k_a indicate strong binding between ARS and alkyloxypyridinium surfactants and comparatively higher value of k_a is obtained for ARS-[HEC_{16}OPyBr]. These may be due to cation-π interactions between pyridinium cation and aromatic group of anthraquinone moiety and π-π interactions among aromatic systems of the two participants [40]. However, the existence of such interactions is fairly justified by ^{1}H-NMR measurements (discussed later). The binding constant values evaluated from both of the studies (UV-visible and voltammetry) complement well each other.

3.4.2 Potentiometric measurements

The cationic alkyloxypyridinium surfactants based ion-selective electrodes respond precisely and particularly to the surfactant ion monomers. As a result, using this characteristic of ion-selective electrodes, these are used to investigate the interactions between dye, ARS and alkyloxypyridinium surfactants; [HEC_{14}OPyBr] and [HEC_{16}OPyBr]. The plots showing the variation of electromotive force (EMF) *versus* logarithm of molar concentration of [HEC_{14}OPyBr] and [HEC_{16}OPyBr] in the absence and presence of ARS at 0.02 mmol dm^{-3} concentration are presented in Fig.7(A) and Fig.S7(A) (supporting information) respectively. Owing to the exquisite reproducibility of the EMF values in the absence of dye at different concentrations of alkyloxypyridinium surfactants, these plots served as calibration curves.

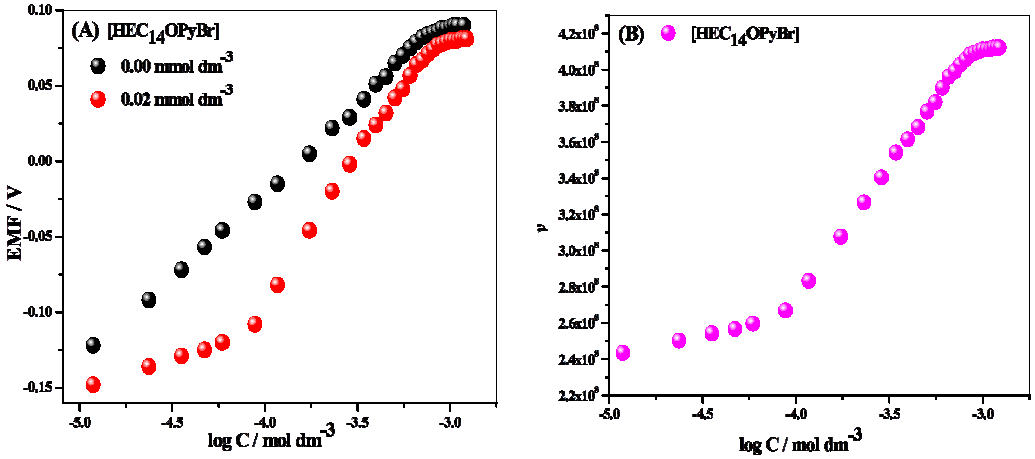

Fig.7 (A) EMF as a function of logarithm of molar concentration of alkyloxypyridinium surfactant, [HEC_{14}OPyBr] in the absence and presence of 0.02 mmol dm^{-3} ARS (B) Binding isotherms of binding parameter (v) *versus* logarithm of molar concentration of [HEC_{14}OPyBr] in the presence of 0.02 mmol dm^{-3} ARS.

The calibration curve is linear over the concentration range of surfactants *i.e.* below the *cmc* (0.00-0.50 mmol dm^{-3} for ([$HEC_{14}OPyBr$] and 0.00-0.12 mmol dm^{-3} for [$HEC_{16}OPyBr$]) with a good slope that is in well agreement with Nernstian response. Any deviation of EMF from the calibration curve in the presence of ARS indicates that the binding of surfactants and ARS takes place. The decrease in EMF values in the presence of dye could be due to the reason that in ARS solution, some of dye molecules bind to the surface of membrane which reduces the potential and it leads to lesser solubilization of the surfactant present in reference solution in the membrane which produces small EMF. It is clear from Fig.7(A) and Fig.S7(A) (supporting information) that binding occurs among ARS and alkyloxypyridinium surfactants even at very low concentration of surfactants and it continues till the dye gets saturated with the monomers of surfactants and then, the curve merges with the calibration curve. Initially, with the addition of surfactant in the form of monomers, potential increases very slightly and thereafter, it increases sharply. The point of intersection of the changes gives a transition C_1 which corresponds to the formation of ion-pairs between oppositely charged dye and surfactants molecules due to strong electrostatic forces of attraction as discussed earlier in conductivity measurements. Beyond C_1, EMF increases linearly with relatively large slope and further, it becomes constant and gives second transition *i.e. cmc* where free micelles of surfactants are formed. The concentrations corresponding to different transitions (C_1 and C_2 (*cmc*)) are presented in Table S1 (supporting information) and these values are in excellent agreement with those extracted from conductivity measurements.

3.4.2.1 Binding Isotherm

The change in EMF values in the presence of dye helps to calculate the amount of alkyloxypyridinium surfactant bound to ARS molecules. The average number of alkyloxypyridinium surfactant monomers bound to ARS *i.e.* binding parameter (v) is obtained using the following equation (9) [41]:

$$v = \frac{[Surf]_t - [Surf]_f}{[ARS]_t} \quad (9)$$

Where $[Surf]_t$ and $[Surf]_f$ represent total concentration and free concentration of alkyloxypyridinium surfactants and $[ARS]_t$ denotes the total concentration of ARS. Fig.7(B) and Fig.S7(B) (supporting information) represents the binding isotherm for binding of

[HEC_{14}OPyBr] and [HEC_{14}OPyBr] with ARS. The binding isotherms show different characteristic regions with increasing concentration of alkyloxypyridinium surfactants. From the binding curve, it is clear that initially, there is small increase in binding which is followed by a sharp increase owing to the complexation between negatively charged dye monomers and cationic alkyloxypyridinium surfactants. Thereafter, binding isotherm acquires constancy and free monomer concentration of surfactants increases until it reaches *cmc*. The transition concentrations corresponding to different binding regions significantly correlates with other techniques studied.

3.5 Morphology of ARS-surfactant mixed aggregates

To get further insights in the structural aspects of ARS-surfactant mixed systems, dynamic light scattering measurements (DLS) have been carried out to gather information about the morphology of ARS-surfactant mixed aggregates. The aggregate size distributions of both pure [HEC_{14}OPyBr] and [HEC_{16}OPyBr] at concentration of 10 times their *cmc* (8.9 mmol dm^{-3} for [HEC_{14}OPyBr] and 2.0 mmol dm^{-3} for [HEC_{16}OPyBr]) show micelles of hydrodynamic diameter (D_h) 1-2 nm. The aggregate size distribution of ARS-[HEC_{14}OPyBr] and ARS-[HEC_{16}OPyBr] mixed systems with increasing mole fraction of ARS (x_{ARS}) are shown in Fig.8(A) and Fig.8(B) respectively and the corresponding values of hydrodynamic diameters (D_h) obtained are presented in Table S2 (supporting information). The total mixture composition was fixed at 3 mmol dm^{-3}.

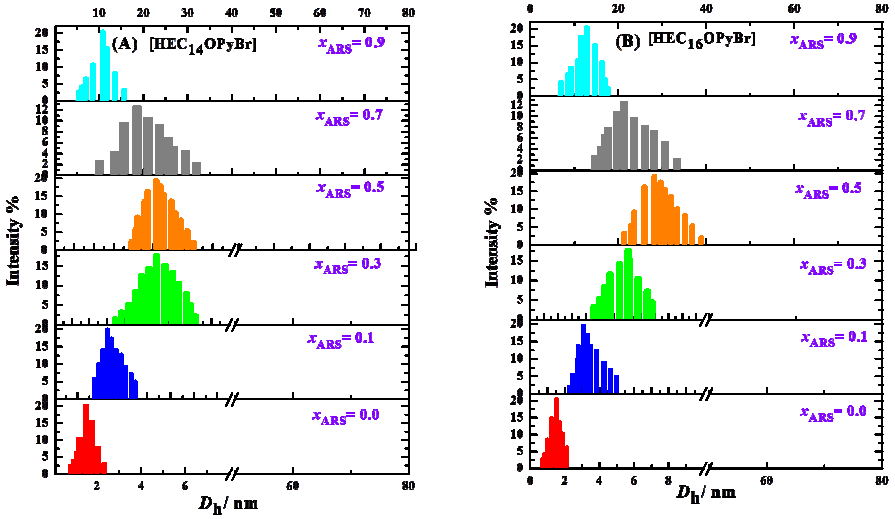

Fig.8 Size distributions for ARS-alkyloxypyridinium surfactant mixtures at varying mole fractions of alkyloxypyridinium surfactants (A) [HEC_{14}OPyBr] (B) [HEC_{16}OPyBr]

A keen analysis of the Table S2 clearly indicates that D_h depends upon the mixture composition and shows a transition from surfactant dominated to ARS dominated mole fractions. In alkyloxypyridinium surfactant dominated mole fractions, D_h of [HEC_{14}OPyBr] surfactant micelles firstly increases from 1.2 nm to 28.5 nm due to intercalation of oppositely charged dye monomers that decreases the electrostatic repulsions between the head groups. As already discussed in surface tension studies, the oppositely charged dye monomers behave as aromatic anions and thus, it leads to formation of bigger micelles with large D_h. Further, in ARS-dominated mole fractions, increase in concentration of ARS cause steric and electrostatic repulsions which breakdown the micelles to smaller sizes and thus, D_h decreases (from 28.5 to 10.5 nm). In ARS-[HEC_{16}OPyBr] mixed system, similar changes have been observed but comparatively larger aggregates are formed. This also supports the importance of hydrophobic interactions in addition to electrostatic interactions in the binding process of ARS and alkyloxypyridinium surfactants.

3.6 Proposed dye-surfactant interaction mechanism by ^{1}H-NMR measurements

The ^{1}H-NMR measurements provide direct indication of the interactions taking place between the two components of a system. For this, the ^{1}H-NMR spectra of 1.0 equivalent of ARS is recorded in CD_3CN solvent and titrated against increasing equivalents of [HEC_{14}OPyBr] and [HEC_{16}OPyBr]. The structures of alkyloxypyridinium surfactant [HEC_{14}OPyBr] and ARS with the numbering assigned to different protons are given as Fig.S8 (supporting information). The effect of increasing equivalents of [HEC_{14}OPyBr] and [HEC_{16}OPyBr] on the δ values of alkyloxypyridinium surfactants is given as supporting information (Table S3 and S4) and the changes are shown in Fig.9(A) and Fig.S9 (supporting information). The remarkable changes in the values of chemical shifts (δ) of ARS and alkyloxypyridinium surfactants help to understand the interaction mechanism among them. The upfield and downfield shifts observed in the ^{1}H-NMR titrations of ARS with increasing equivalents of [HEC_{14}OPyBr] indicates the existence of cation-π interactions among them. Literary also revealed the existence of cation-π interactions among the pyridinium cation and delocalized π electron cloud of an aromatic ring [40,42,43]. The aromatic protons of ARS are shifted downfield indicating polar medium on the micellar interface. It suggests that the dye monomers behave as aromatic anions and stays in the palisade layer of alkyloxypyridinium surfactants. These results are also confirmed by the decrease in *cmc*

values of [$HEC_{14}OPyBr$] and [$HEC_{16}OPyBr$] as observed in surface tension, conductivity and potentiometric measurements. However, the hydroxyl group at 2nd position (according to IUPAC name of ARS) show upfield shift due to interactions with alkyloxypyridinium surfactants. But the hydroxyl at 1st position donot show any downfield or upfield shift [Fig.9(B)].

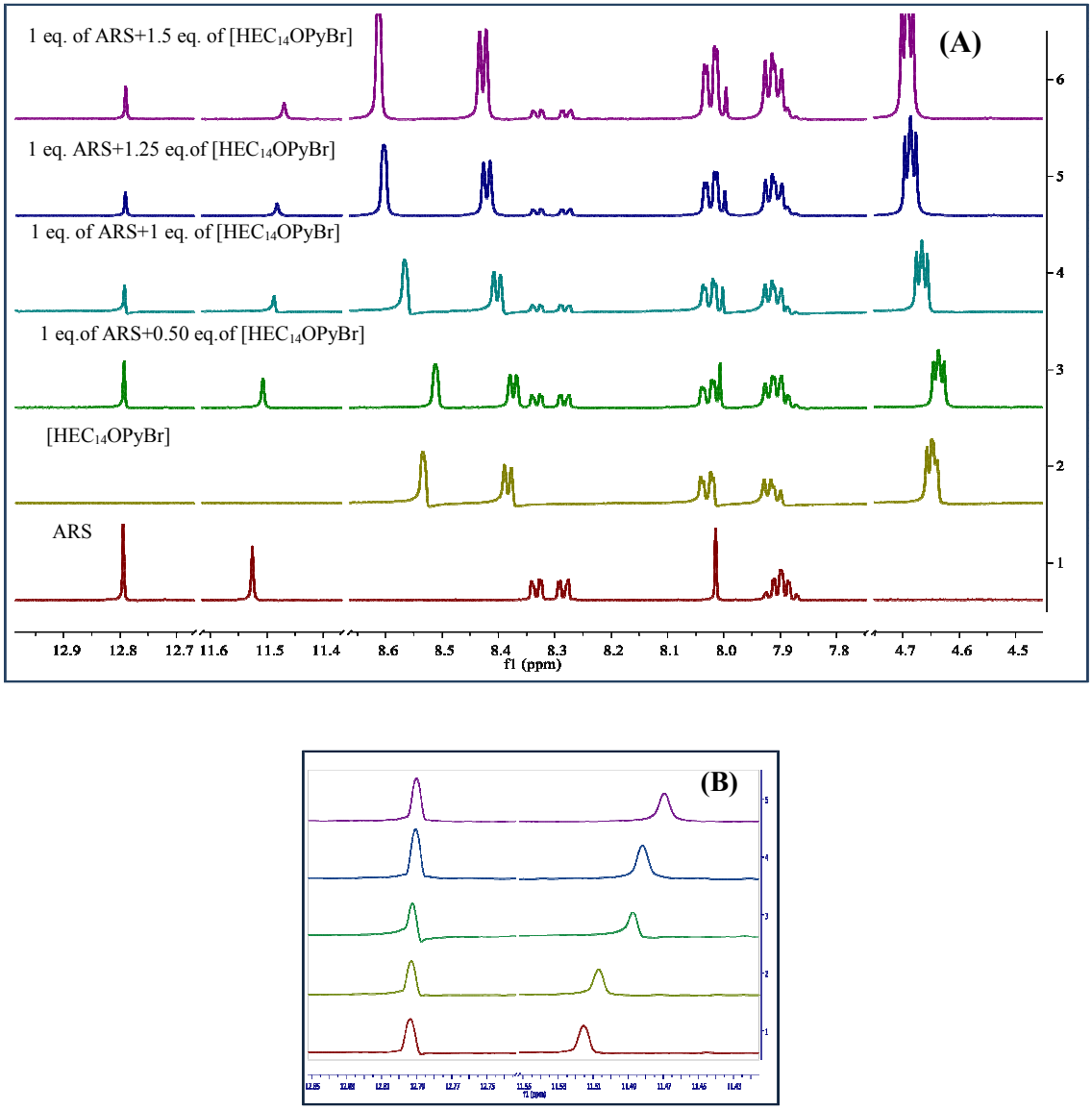

Fig.9 (A) ^{1}H-NMR titrations of ARS with increasing equivalents of alkyloxypyridinium surfactant [$HEC_{14}OPyBr$] (B) Chemical shift changes in the region of hydroxyl group moiety of ARS with increasing equivalents of [$HEC_{14}OPyBr$]

Similar trends in chemical shifts have been observed in ARS-[$HEC_{16}OPyBr$] mixed system. These results clearly indicate that one of the hydroxyl groups is involved in the interaction mechanism and the other is involved in intramolecular hydrogen bonding with the neighbouring carbonyl group. These results are in accordance with the voltammetric measurements where prominent changes occur due to oxidation of catechol moiety. As a result, these studies confirm that predominantly, the catechol moiety of ARS interacts with the alkyloxypyridinium surfactants. Moreover, the presence of ARS greatly affects the environment of protons of alkyloxypyridinium surfactants especially the protons in close proximity of pyridinium cation head group leading to downfield shift of these protons. Hence, the results from ^{1}H-NMR measurements highlight the role of cation-π and H-bonding interactions in addition to hydrophobic and electrostatic interactions between ARS and alkyloxypyridinium surfactants.

3.7 Conclusions

In view of the diverse applications of dye-surfactant mixed systems, the present work aims to explore the basic understanding of the interactions among oppositely charged dye and surfactant molecules. An estimation of such interactions is very much essential from environmental point of view, as the surfactants are being used in different ways to remove toxic dyes from waste water such as by enhanced micellar ultrafiltration, surfactant mediated cloud point extraction. The surfactants are also used to modify alumina so as to increase its absorption efficiency to remove harmful dyes. To the best of our knowledge, there is no report in the literature dealing with the studies of interactions between anionic redox-active dye, alizarin red S and alkyloxypyridinium surfactants using multi-technique approach. The surface tension and conductivity studies explores the formation of close packed dye-surfactants ion pair (DSIP) which further leads to the formation of pre-micellar aggregates with the dye molecules behaving as aromatic anions dissolved in the palisade layer. UV-visible and voltammetric measurements reveal the 1:1 stoichiometry of DSIP in the lower concentration regions of surfactants and the higher values of binding constant are attributed to electrostatic, hydrophobic, cation-π and π-π interactions. DLS measurements indicate that the size of ARS firstly decreases due to the formation of close-packed dye-surfactant ion pairs and further increases due to the transformation of these ion-pairs into mixed micelles of alkyloxypyridinium with ARS.

The difference between lower energy HOMO and higher energy LUMO *i.e.* the band gap of ARS decreases by the addition of alkyloxypyridinium surfactants which indicate that the higher energy LUMO gets stabilized due to dye-surfactant complex formation. This charge transfer mechanism is responsible for large bathochromic shift of 130.5 nm in the absorption spectra of ARS. Voltammetry also supports these results as the oxidation peak due to oxidation of catechol moiety (P_3) exhibits anodic shift on addition of surfactants. The calculated electrochemical parameters like diffusion coefficient (D), formal potential ($E°$), electron transfer coefficient (α) and surface reaction rate constant (k_s) of ARS decrease in the presence of surfactants which reveal the formation of non-electroactive dye-surfactant complex responsible for the decrease in peak current intensity associated with anodic shift. The results extracted from ^{1}H-NMR confirms the complexation mechanism *i.e.* the hydroxyl group moiety of ARS interacts with the neighbouring protons of pyridinium cationic head-group of alkyloxypyridinium surfactants by virtue of cation-π, electrostatic and hydrophobic interactions and these results corroborates well with voltammetry.

Acknowledgement

This work was financially supported by the Department of Science and Technology (DST) New Delhi, India as a part of Project NO.SR/S1/PC-02/2011. Renu Sharma is thankful to the Council of Scientific and Indian Research (CSIR), New Delhi, India, for the award of Senior Research Fellowship.

References

1) S. Safavi, H. Abdollahi, N. Maleki, S. Zeinali, Interaction of anionic dyes and cationic surfactants with ionic liquid character. *J. Colloid Interface Sci.* 2008, **322**, 274-280.
2) O. Duman, S. Tunc, B. Kanc, Spectroscopic studies on the interactions of C.I. Basic Red 9 and C.I. Acid Blue 25 with hexadecyltrimeythylammonium bromide in cationic surfactant micelles. *Fluid Phase Equilib.* 2011, **301**, 56-61.
3) A. A. Shahir, S. Javadian, B. B. M. Razavizadeh, Comprehensive study of tartrazine/cationic surfactant interaction. *J. Phys. Chem. B.* 2011, **115**, 14435-14444.
4) Y. P. Chin, F. A. R. Raof, S. Sinniah, V. S. Lee, S. Mohamad, N. S. A. Manan, Inclusion complex of alizarin red s with β-cyclodextrin: synthesis, spectral, electrochemical and computational studies. *J. Mol. Struct.* 2015, **1083**, 236-244.
5) S. Jagadeeswari, M. A. Jhonsi, A. Kathivaran, R. Renganathan, Photoinduced interaction between MPA capped CdTe QDs and certain anthraquinone dyes. *J. Luminiscence* 2011, **131**, 597-602.
6) A. M. Faouzi, B. Nasr, G. Abdellatif, Electrochemical degration of anthraquinone dye alizarin red s by anodic oxidation on boron doped diamond. *Dyes Pigments* 2007, **73**, 86-89.
7) P. Zucca, C. Vinci, F. Sollai, A. Rescigno, E. Sangust, Degradation of alizarin red s under mild condition by immobilized 5,10,15,20-tetrakis (4-sulfonatophenyl) porphin-Mn(III) as a biomimetic peroxidase-like catalyst. *J. Mol. Catal. A: Chem*. 2008, **288**, 97-102.
8) S. Ito, T. Miyoshi, Microscopic observations on tissue calcium distribution in the brown alga, undaria pinnatifida (Harvey) suringar. *J. App. Phycol.* 1993, **5**, 15-21.
9) F. R. Zaggout, A. E. F. A. Qarraman, S.M. Zourab, Behavior of immobilized alizarin red s into sol-gel matrix as a pH-sensor. *Mater. Lett*. 2007, **61**, 4192-4195.
10) Y. Kubo, T. Ishida, A. Kobayashi, T. D. James, Fluorescent alizarin-phenylboronic acid acid ensembles: design of self-organized molecular sensors for metal ions and anions. *J. Mater. Chem.* 2005, **15**, 2889-2895.
11) I. Sahin, N. Nakiboglu, Voltammetric determination of boron by using alizarin red s. *Anal. Chim. Acta* 2006, **572**, 253-258.

12) M. J. Ruedas Rama, A. Ruiz Medina, A. Molina Diaz, A flow-injection renewable surface sensor for the fluorimetric determination of vanadium (V) with alizarin red s. *Talanta* 2005, **66**, 1333-1339.

13) S. A. Shama, A. S. Amin, Determination of proteins with alizarin red s by rayleigh light scattering. *Spectrochimica Acta A* 2004, **60**, 1769-1774.

14) H. Zhong, N. Li, F. Zhao, K. A. Li, Spectrophotometric determination of nefopam, mebevrine and phenylpropanolamine hydrochloride in pharmaceutical formuations using alizarins. *Talanta* 2004, **62**, 37-42.

15) P. Pandit, S. Basu, Removal of ionic dyes from water by solvent extraction using reverse micelles. *Environ. Sci. Technol*. 2004, **38**, 2435-2442.

16) M. N. Khan, A. Sarwar, Study of dye-surfactant interaction: aggregation and dissolution of yellowish in N-dodecyl pyridinium chloride. *Fluid Phase Equilib*. 2006, **239**, 166-171.

17) R. Sanan, T. S. Kang, R. K. Mahajan, Complexation, dimerization and solubilization of methylene blue in the presence of biamphiphilic ionic liquids: a detailed spectroscopic and electrochemical study. *Phys. Chem. Chem. Phys.* 2014, **16**, 5667-5677.

18) I. N. Kurniasih, H. Liang, P. C. Mohr, G. Khot, J. P. Rabe, A. Mohr, Nile red dye in aqueous surfactant and micellar solution. *Langmuir* 2015, **31**, 2639-2648.

19) B. Simoncic, M. Kert, Thermodynamics of anionic dye-cationic surfactant interactions in cationic-nonionic surfactant mixtures in comparison with binary mixtures. *Dyes Pigments* 2006, **71**, 43-53.

20) F. Gul, A. M. Khan, S. S. Shah, F. N. Nazar, Spectroscopic study of alizarin red s binding with cetyltrimethylammonium bromide at low concentrations. *Color. Technol*. 2010, **126**, 109-113.

21) M. J. Rosen, *Surfactants and interfacial phenomenon*, third ed. Wiley-Interscience, New York, 2004.

22) D. Blunk, P. Bierganns, N. Bongartz, R. Tessendorf, C. Stubenrauch, New speciality surfactants with natural structural motifs. *New J. Chem*. 2006, **30**, 1705-1717.

23) S. Bhattacharya, J. Haldar, Microcalorimetric and conductivity studies with micelles prepared from multi-headed pyridinium surfactants. *Langmuir* 2005, **21**, 5747-5751.

24) A. Cornelles, L. Perez, F. Comelles, I. Ribosa, A. Manresa, M. T. Garcia, Self-aggregation and anti-microbial activity of imidazolium and pyridinium based ionic liquids in aqueous solution. *J. Colloid Interface Sci*. 2011, **355**, 164-171.

25) V. Chauhan, S. Singh, R. Kamboj, R, Mishra, G. Kaur, Synthesis, micellization properties, and cytotoxicity trends of N-hydroxyethyl-3-alkyloxypyridinium surfactants. *Colloid Polym. Sci*. 2014, **292**, 467-476.

26) A. Ali, S. Uzair, N. A. Malik, M. Ali, Study of interaction between cationic surfactants and cresol red dye by electrical conductivity and spectroscopy methods. *J. Mol. Liq.* 2014, **196**, 395-403.

27) M. J. Rosen, *Surfactant and Interfacial Phenomenon*, 2nd edn; John Wiley and Sons: New York, 1988.

28) R. Sharma, A. Kamal, T. S. Kang, R. K. Mahajan, Interactional behavior of polyelectrolyte poly sodium 4-styrene sulphonate (NaPSS) with imidazolium based surface active ionic liquids in aqueous medium. *Phys. Chem. Chem. Phys*. 2015, **17**, 23582-23594.

29) B. Gohain, S. Sarma, R.K. Dutta, Protonated dye-surfactant ion pair formation between neutral red and anionic surfactants in aqueous submicellar solutions. *J. Mol. Liq.* 2008, **142**, 130-135.

30) B. Gohain, R. K. Dutta, Premicellar and micelle formation behavior of dye surfactant ion pairs in aqueous solutions: deprotonation of dye in ion pair micelles. *J. Colloid Interface Sci.* 2008, **323**, 395-402.

31) R. T. Buwalda, J. M. Jonker, J. B. F. N. Engberts, Aggregation of azo dyes with cationic amphiphiles at low concentrations in aqueous solution. *Langmuir* 1999, **15**, 1083-1089.

32) S. Mondal, B. Doloi, S. Ghosh, Spectroscopic studies of interaction of safranine T with ionic surfactants. *Fluid Phase Equilib*. 2013, **360**, 180-187.

33) S. Gokturk, M. Tuncay, Dye-surfactant interaction in the pre-micellar region. *J. Surf. Deterg*. 2003, **6**, 325-330.

34) A. Kamal, R. Raj, V. Kumar, R. K. Mahajan, Highly selective amide-tethered 4-aminoquinoline-lactum based electrochemical sensors for Zn (II) ion recognition. *Electrochimica Acta* 2015, **166**, 17-25.

35) S. Schumacher, T. Nagel, F. W. Scheller, N. Gajovic-Eichelmann, Alizarin red s as an electrochemical indicator for saccharide recognition. *Electrochimica Acta* 2011, **56**, 6607-6611.

36) M. P. Soriaga, A. T. Hubbard, Determination of the orientation of adsorbed molecules at solid-liquid interfaces by thin-layer electrochemistry: aromatic compounds at platinum electrodes. *J. Am. Chem. Soc.* 1982, **104**, 2735-3742.

37) J. Tauc, Optical properties and electronic structure of amorphous Ge and Si. *Mater. Res. Bull.* 1968, **3**, 37-46.

38) K. Chokshi, S. Qutubuddin, A. Hussam, Electrochemical investigation of microemulsions. *J. Colloid Interface Sci*. 1989, **129**, 315-326.

39) X. Hu, K. Jiao, W. Sun, J. Y. You, Electrochemical and spectroscopic studies on the interaction of malachite green with DNA and its application. *Electroanalysis* 2006, **18**, 613-620.

40) R. K. Mahajan, S. Mahajan, A. Bhadani, S. Singh, Physicochemical studies of pyridinium gemini surfactants with promethazine hydrochloride in aqueous solution. *Phys. Chem. Chem. Phys.* 2012, **14**, 887-898.

41) A. K. Bordbar, A. Taheri-Kafrani, Binding and fluorescence study on interaction of human serum albumin (HSA) and cetylpyridinium chloride (CPC). *Colloids Surf. B* 2007, **55**, 84-89.

42) E. V. Pletneva, A. T. Laederach, D. B. Fulton, N. M. Kostic, The role of cation−π interactions in biomolecular association. design of peptides favoring interactions between cationic and aromatic amino acid side chains. *J. Am. Chem. Soc.* 2001, **123**, 6232-6245.

43) Y. Huang, Y. Jiang, S. D. Bull, J. S. Fossey, T. D. James, Diols and anions can control the formation of an exciplex between a pyridinium boronic acid with an aryl group connected *via* a propylene linker. *Chem. Comm*. 2010, **46**, 8180-8182.